Journal of Instrumentation

SISSA

PAPER • OPEN ACCESS

Silicon strip defects and their impact on electrical performance of readout electronics

To cite this article: A. Affolder *et al* 2021 *JINST* **16** P03037

Published by IOP Publishing for Sissa Medialab

Received: *December 24, 2020*
Accepted: *February 3, 2021*
Published: *March 24, 2021*

Silicon strip defects and their impact on electrical performance of readout electronics

A. Affolder,[a] V. Fadeyev,[a] Z. Galloway,[a] M. Gignac,[a,*] J. Gunnell,[a] J. Johnson,[a] N. Kang,[a] J. Kaplon[b] and F. Martinez-Mckinney[a]

[a] *University of California Santa Cruz,*
1156 High St, Santa Cruz, CA, U.S.A.
[b] *CERN,*
Espl. des Particules 1, 1211 Meyrin, Switzerland

E-mail: matthew.gignac@cern.ch

Abstract: In preparation for the High Luminosity LHC (HL-LHC) runs, the ATLAS inner detector will be completely replaced with an all silicon Inner Tracker (ITk). Hybrid silicon pixel modules will be used for the innermost tracking layers, and silicon micro-strip detectors will be used the outer layers of the tracker. During the production of the detector, the sensors, readout electronics, and other components will undergo a series of quality control (QC) and quality assurance tests. Defects in the fabrication of the sensors will be flagged early in the manufacturer's and ATLAS QC tests. A study of the influence of sensor defects was performed to assess the characteristics of these defects in completed modules, and whether any defect posed a risk to the operation of the front-end readout electronics. All defects were found to have no impact on the performance of the front-end readout electronics for healthy amplifier channels, and defects that short the coupling between the strip implant and the metal readout electrode were only noticeable for strip leakage currents in excess of 250 nA, beyond the end-of-life currents expected for most sensors at the HL-LHC.

Keywords: Detection of defects; Front-end electronics for detector readout; Radiation-hard detectors; Si microstrip and pad detectors

*Corresponding author.

https://doi.org/10.1088/1748-0221/16/03/P03037

2021 JINST 16 P03037

Contents

2021 JINST 16 P03037

1 Introduction

The ATLAS detector will be upgraded in preparation for the High Luminosity LHC (HL-LHC) in order to cope with instantaneous luminosities up to $7.5{\times}10^{34}\,\mathrm{cm}^{-2}\,\mathrm{s}^{-1}$ and an average number of proton-proton collisions per bunch cross, $\langle\mu\rangle$, of up to 200. As part of these upgrades, the inner detector will be completely replaced by the all silicon Inner Tracker (ITk) [1, 2]. The ITk will use hybrid silicon pixel modules for the inner most barrel and end-cap layers, surrounded by silicon micro-strip modules at larger radii.

At the end of life, the ITk silicon micro-strip detector will be exposed to an equivalent 1 MeV neutron fluence ($n_{\mathrm{eq}}/\mathrm{cm}^2$) of up to $1.6 \times 10^{15}\,n_{\mathrm{eq}}/\mathrm{cm}^2$ and an ionizing dose of 0.66 MGy, giving rise to sensor leakage currents in the range of 100–200 nA per strip. For these large sensor currents, it is crucial to understand the effects that various sensors defects have on the front-end readout electronics. A particularly important type of defect that shorts the capacitor between the strip implant and the metal readout electrode is called "pinholes" in this paper [3, 4]. As a result of the short, the implant becomes directly connected to the amplifier's input, which could dump large leakage currents into the front-end electronics, potentially destroying the functionality of the chip as a whole. This would give rise to large holes in the tracking detector acceptance and severely impact the performance of the detector as a whole.

Pinhole channels could arise during sensor production or throughout the module assembly process, but are expected to happen rarely. In addition to the production and assembly process, during operation the sensors could be damaged by a large flux of charged particles, many orders of magnitude greater than the operational conditions. Such a scenario may occur when the HL-LHC beam is mis-steered and hits beam collimators or other structures, depositing a large amount of ionization in the innermost detectors. Due to the large ionization in the sensor volume and the resulting current through the bias resistors, the strip implants may acquire a large potential, imposing high voltage on the coupling capacitors and potentially damaging them. There are several design features

implemented in the sensors and modules to counteract such phenomenon. The coupling capacitors are specified to tolerate up to 100 V.[1] The sensor layout uses specialized Punch-Through Protection (PTP) structures to keep the strip implants potential low [6], to protect the AC-coupling capacitors from large charge accumulation [7]. Finally, the simulations in ref. [5] indicate the importance of the module high voltage filter and the high voltage powering. If the onset of the beam loss is slow enough, the charge present on the filter capacitor gets depleted, naturally removing high voltage and the damage possibility from a module. If, in spite of all these precautions, the damage still occurs, the pinhole impact on the system performance becomes relevant in such an operational context.

In this paper, we investigate the effects that pinholes and other defects in silicon strip sensors have on the performance of the front-end (FE) readout electronics, and our ability to flag these defects during electrical tests performed during the assembly process. This is an additional layer of QC assessment that may help if something is missed during the manufacturer or sensor QC tests, or, more likely, if there are new defects created during the module assembly or handling. We show that pinhole channels for unirradiated sensors do not impact the electrical characteristics of the chip, and only after irradiation when the leakage current per strip is above at least 250 nA do the pinholes have a measurable effect on the channel. Moreover, we show that the neighbouring channels are unaffected by the presence of the pinhole channel, demonstrating that these electrical shorts do not pose any risk to the operation of the chip as a whole.

2 Experimental setup

In order to study the effects of sensor defects on the electrical performance of the readout chips, full sized modules and a custom setup with miniature prototype sensors and readout chips were studied. Individual sensor strips were connected to readout chip channels with 25 µm Aluminum wire using an ultrasonic wire-bonding process. Simulated sensor defects were intentionally added to the sensors through a wire-bonding process as described in the next section. Both non-irradiated and proton/neutron irradiated sensors were studied at a variety of temperatures.

2.1 Silicon micro-strip sensors

In this study, silicon micro-strip sensors from the so-called ATLAS17LS submission [8] were used.[2] These sensors were manufactured by Hamamatsu Photonics K. K (HPK) as part of a large market survey to find sensor suppliers for both the ATLAS and CMS detector upgrades in preparation for the HL-LHC phase. The sensors are 320 µm thick single-sided micro-strip sensors made with n^+-strips implanted on p-type silicon bulk. The strip implants have poly-silicon biasing resistors. They are AC-coupled to the readout electrodes. Sensors were fabricated onto wafers. Each wafer contained full sized sensors with strip lengths measuring 4.84 cm, and miniaturized sensors along the periphery with shorter strip lengths. The miniaturized sensors used in this study measured 1×1 cm^2 in physical size with 0.8 cm long strip lengths. Full sized sensors and miniaturized sensors were used to study the electrical characteristics of defects.

[1] The higher this value, the more protection the coupling capacitors have in the beam loss scenario. The value was chosen based on manufacturability considerations and the fact that it was found to be adequate in a previous simulation of a module response [5].

[2] No technological changes between these sensors and the final version are expected for the ITk strip detector.

2021 JINST 16 P03037

The miniaturized sensors were irradiated with 70 MeV protons at the Cyclotron and Radioisotope Center (CYRIC) of Tohoku University in Japan. During the proton irradiation, the sensors were kept inside a box cooled down to −15 °C. The beam scanned the full length of the sensor to ensure the entire sensor was irradiated. Neutron irradiations on miniaturized sensors were performed at the Ljubljana TRIGA Reactor at the Jožef Stefane Institute [9]. The temperature of the samples was observed to reach about 40 °C. The total fluence for both the proton and neutron irradiated sensors was 1×10^{16} n_{eq}/cm^2. The full sized sensors in this study were not irradiated.

The sensors were cooled to reduce the leakage current during the tests. The miniaturized sensors were biased at $V_b = -100$ V, while the full sized sensors were biased at their nominal value of $V_b = -400$ V. An external chiller pumped deionized coolant through an aluminum jig in thermal contact with the backside of the sensors. Thermal tape was applied between the interface of the aluminum jig and the backside of the sensor support structure for the miniaturized sensor setup. The sensors and aluminum jig were isolated from the environment and continuously flushed with dry air to keep the relative humidity below 10%. Operating temperatures between +12 °C and −15 °C were studied.

Throughout the sensor prototyping rounds, most sensors had a small number of defects, or none at all [10, 11]. In order to study the effects of strip defects on the readout electronics, strip defects were intentionally added by coupling individual strips on the sensor in four configurations. Connections between the pads was accomplished through wire-bonding as pictured in figure 1, and are defined as:

- **DC-to-AC**. The AC and DC bond pads on a single strip were directly connected to simulate a pinhole.
- **DC-to-DC**. The DC bond pads on neighbouring sensor pads were directly connected to simulate an implant short on the sensor.
- **AC-adjacent short**. The AC pads on neighbouring pads were connected to simulate a metal strip short on the sensor.
- **AC-next neighbour short**. The AC pads on next-to-neighbouring pads were connected to simulate a short from touching wire-bonds connecting the front-end readout chips to the sensor.

2.2 Readout chips

The ATLAS Binary Chip with Star readout (ABCStar) and Hybrid Controller Chip (HCCStar) are the front-end readout chips for the ITk strip modules. The ABCStar consists of 256 readout channels with preamplifier-shapers followed by discriminators with individual trimming capabilities. The HCCStar acts as the interface between the ABCStar chips and the module readout system. During the module tests, signals from the HCCStar are routed onto a FR4 readout panel board before being processed by an FPGA board with custom firmware and forwarded over ethernet to the final readout computer for data analysis. For a more detailed description of the prototype chip sets, the reader is directed to ref. [12].

2021 JINST 16 P03037

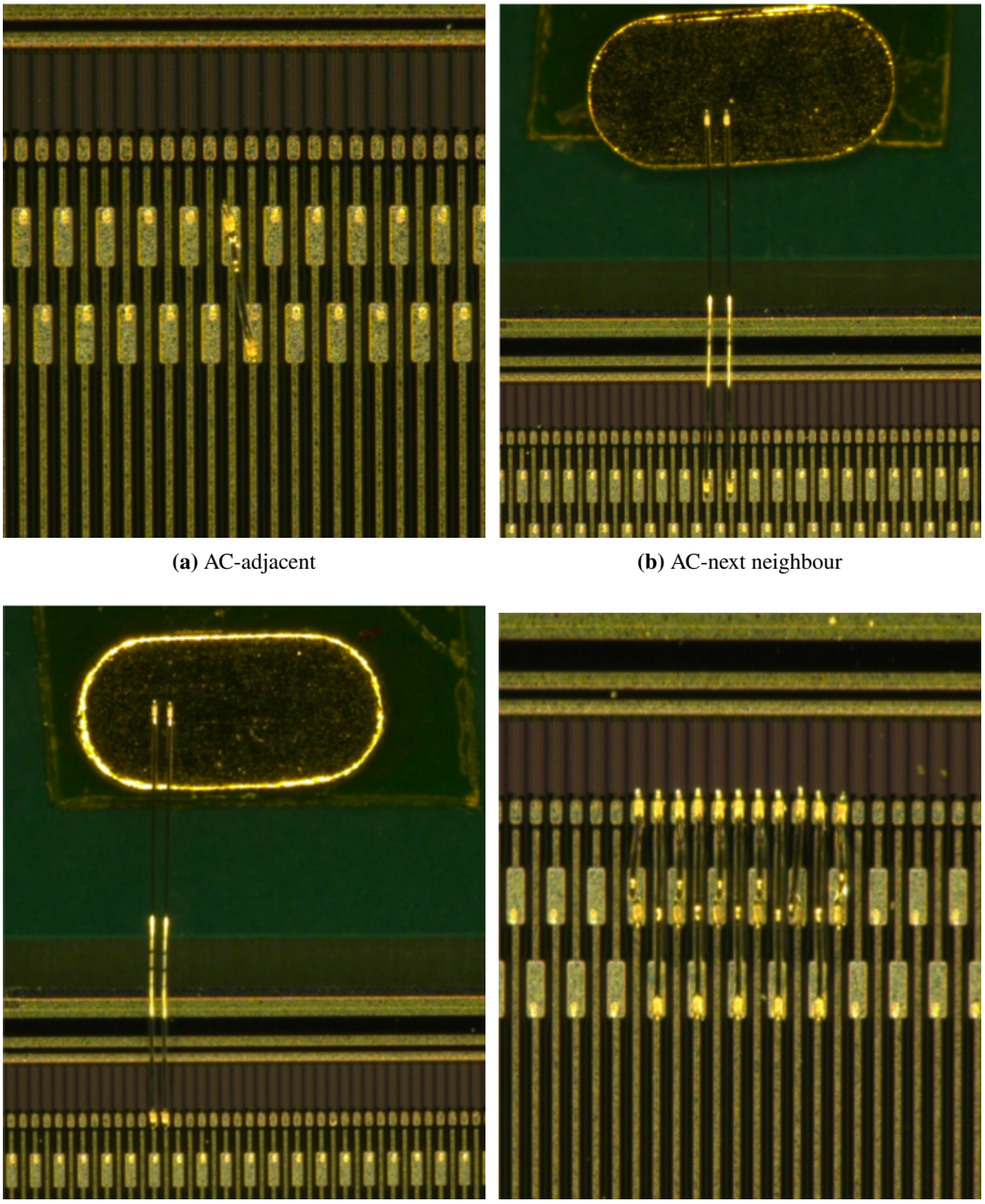

(a) AC-adjacent

(b) AC-next neighbour

(c) DC-to-DC

(d) DC-to-AC

Figure 1. Sensor defects were simulated by wire-bonding the AC and/or DC pads of individual strips as shown in the images. The AC pads are the relatively larger rectangular pads meant for strip signal readout and testing, while the DC pads are the smaller square pads closer to the bias resistors meant for sensor testing only.

2021 JINST 16 P03037

For the full sized sensor, a full module was constructed with ten ABCStar chips and a single HCCStar chip. The assembly procedures follow closely those described in ref. [13]. For the miniaturized sensors, four ABCStar chips and one HCCStar chip were glued onto a prototype hybrid made of low-mass flexible copper-polyimide PCB. Similar to the module assembly procedure, electrical connections between the hybrid and chips, and the chips and sensor strips were established through a wire-bonding process. Each miniature sensor has 104 strips and thus only 104 of the available 256 readout channels were bonded and used for study. The final wire-bonded setup with all four chips is shown in figure 2.

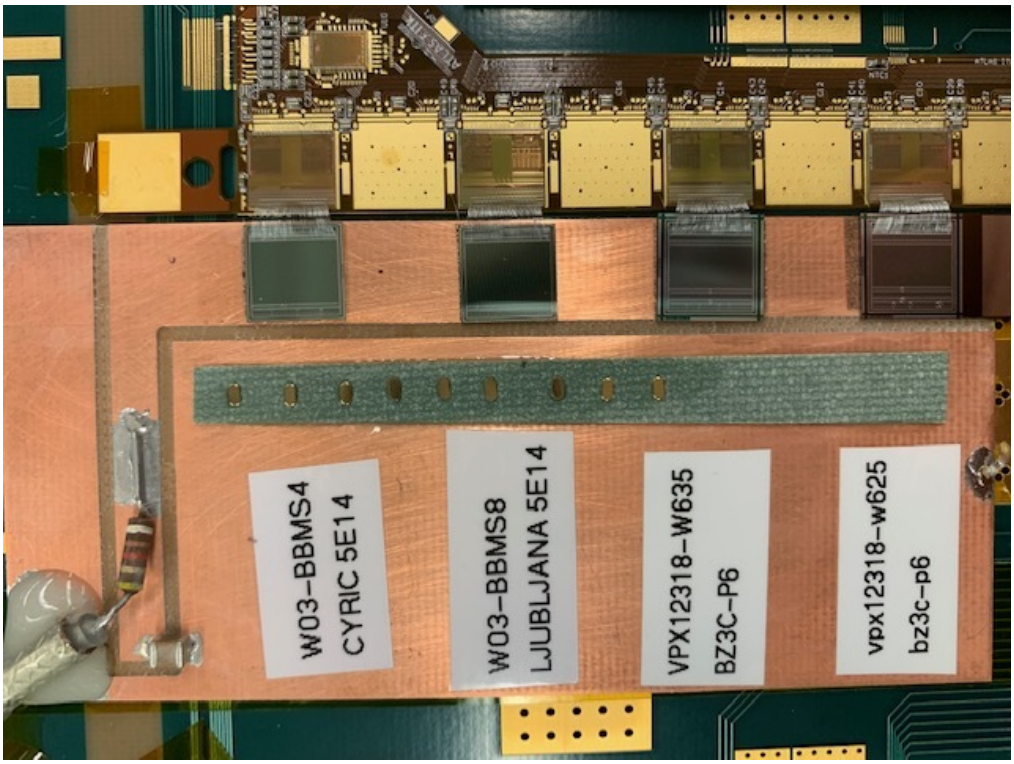

Figure 2. An image of the sensors bonded to ABCStar readout chips. The HCCStar is the smaller chip in the top portion of the picture.

3 Results

3.1 Electrical characteristics

An internal charge injection test from the ABCStar chip is performed to characterize the combined sensor-ASIC performance. Charges of 0.5 fC, 1.0 fC and 1.5 fC were injected into every eighth channel, and the discriminator threshold was scanned resulting in a characteristic "S-curve". The halfway point is termed $V_T(50)$, and the width is a measure of the overall noise. From the linear relationship between $V_T(50)$ and injected charge, the chip gain is derived in units of mV/fC. Chip level averages are calculated by averaging the individual strip gain and noise values, and any channel $> 3\sigma$ from its mean value is flagged as a bad channel.[3]

[3]This is done in an iterative process, so that the bad channel doesn't skew the mean and sigma values.

2021 JINST 16 P03037

The performance of channels without defects was unaffected by the introduction of the defects in other channels for both full sized and miniaturized sensors, signifying that none of the defects posed any risk for the operation of the front-end chip as a whole. All channels with AC-adjacent, AC-next neighbour, and DC-to-DC defects were distinctly visible at all temperatures during the electrical tests. For both AC-adjacent and AC-next neighbour shorted channels, the response shared a common theme where both channels had extremely low gain values (<10 mV/fC) and no measurable noise values, since the response of the channels at small discriminator values went rapidly to zero. The DC-DC connections were characterized as having extremely high noise. Most channels with DC-DC connections had noise measurements 50% higher compared to the values measured before the defect was added.

For channels that had simulated pinholes (DC-AC connections), the response strongly depended on the irradiation history, the operating temperature and thus the strip leakage current. In the full sized unirradiated sensors, pinholes were not visible due to small leakage currents. As shown in figure 3, the pinhole channels in the miniaturized irradiated sensors have a measurable difference in gain values compared to the chip average as a result of the defect. This effect is only visible at higher temperatures when the sensor leakage current is large. At lower temperatures and smaller sensor leakage currents, the pinhole channels are similar to the chip average and impossible to distinguish from a healthy channel.

3.2 Sensor leakage current

Due to its importance for the pinhole effect, the strip leakage current was directly measured using a parameter analyzer between each charge injection test described earlier. On five consecutive strips on each sensor, wire-bonds were added directly to the DC pad and connected for readout to the parameter analyzer. These strips were isolated from the amplifier by the coupling capacitor. The input amplifier of the ABCStar chip operates nominally at $V_{in} = 0.25$ V relative to the hybrid ground. The module powering scheme offsets the sensor reference by $V_{ref} = 0.115$ V relative to the hybrid ground. This results in the amplifier's input being at $\Delta V = V_{in} - V_{ref} = 0.135$ V relative to the sensor bias ring. To find the current flowing between the sensor and the amplifier under such condition, a current-voltage scan was performed between voltages of -0.5 V to $+0.5$ V, and the average of the five measurements were fit with a linear function. The charge injection and sensor current measurements were performed sequentially at the same temperature to maintain the same thermal conditions and therefore the sensor leakage currents. Due to the non-zero potential of the amplifier's input, in the presence of a pinhole the sensor current supplied by amplifier channel consists of two components: the leakage current from the sensor volume subtended by the strip area and the current going through the bias resistor between the sensor bias ring and the amplifier input. The current from the bias resistor was subtracted off so that the measured current values correspond solely to the sensor leakage current. Leakage current values between 100 nA and 500 nA were measured and found to be consistent between proton and neutron irradiated sensors as shown in figure 4.

The temperature vs sensor leakage currents in figure 4 were used to calibrate the charge injection test, such that the measured gain could be studied as a function of the sensor leakage current as shown in figure 5. The gain measurements for all pinhole channels were averaged separately for the neutron and proton irradiated sensors. The measurements are compared against a simulated pinhole setup modeled in SPICE [14], a general-purpose circuit simulation program. The setup

2021 JINST 16 P03037

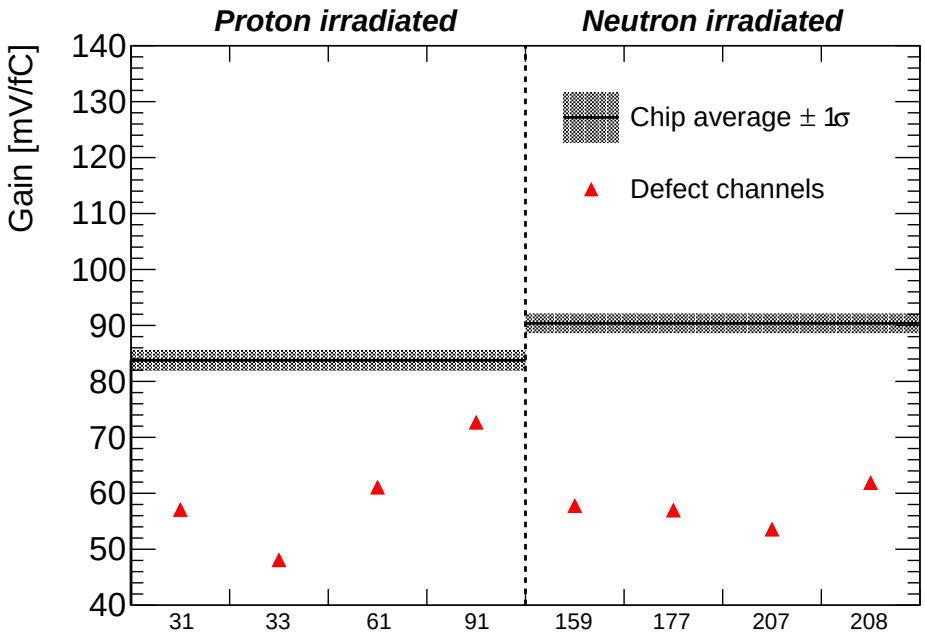

(a) +5 °C

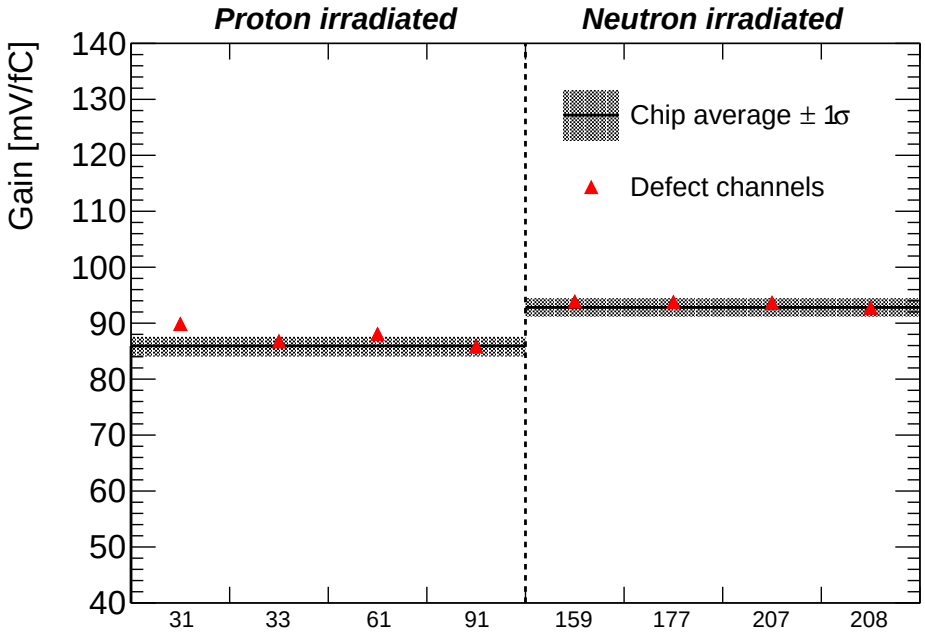

(b) −14 °C

Figure 3. Measured gain values and the corresponding chip average for the neutron and proton irradiated sensors. Only channels numbers with simulated pinhole (AC-DC connections) defects are shown. Gain measurements are shown separately for +5 °C and −14 °C runs.

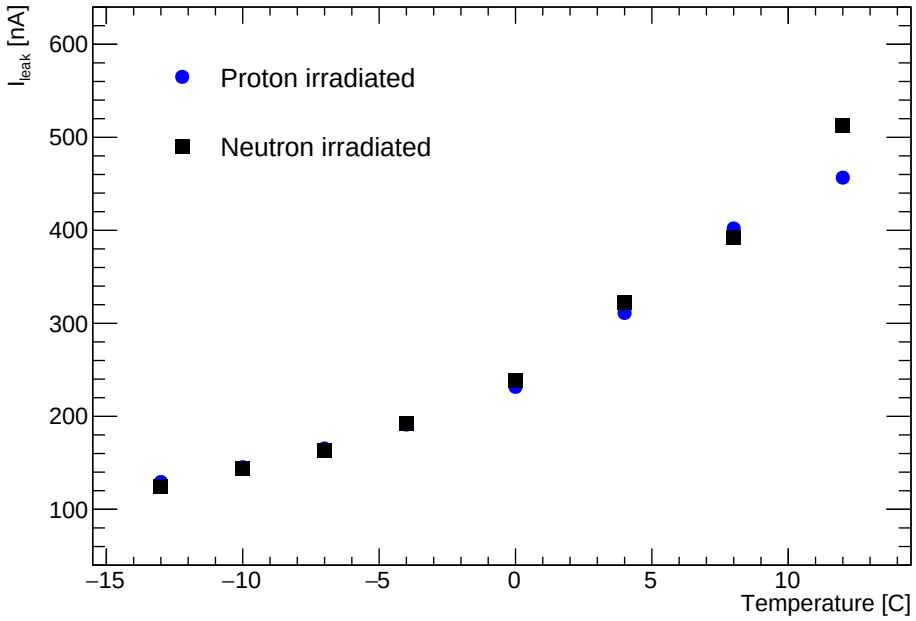

Figure 4. Measured sensor leakage currents as a function of operating temperature for miniaturized proton and neutron irradiated sensors.

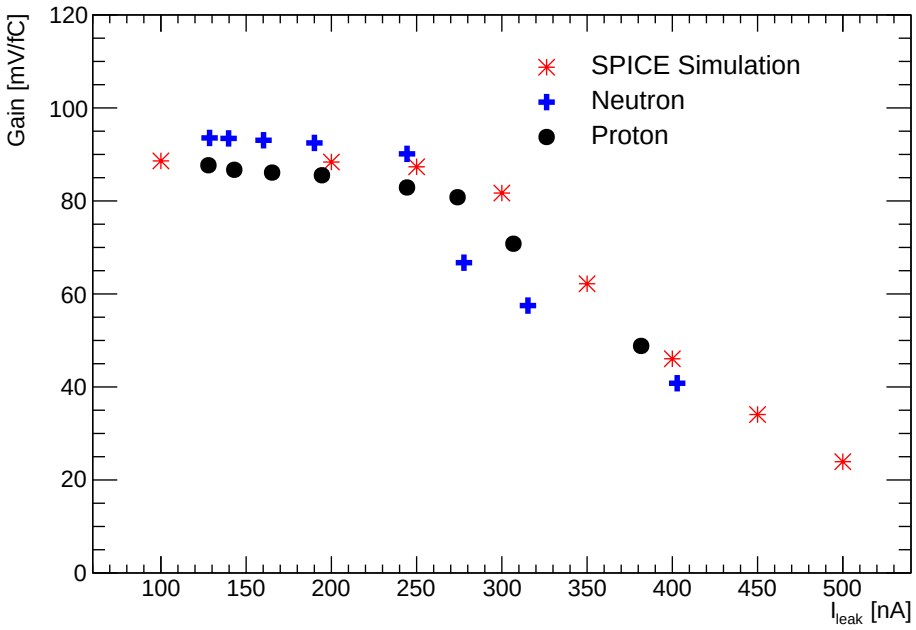

Figure 5. Average gain for pinhole channels as a function of measured leakage current. Results are shown separately for proton and neutron irradiated sensors.

included a complete simulation of the front end channel. Above 250 nA, a visible degradation in the gain is measured and in agreement with the predictions from simulation. The reduction in gain comes from the second stage of the amplifier which is DC coupled to the pre-amplifier output. The feedback resistor in the pre-amplifier has the value of 105 kΩ and the DC drop created by the excess leakage current is amplified by the second stage (DC gain 10V/V). The amplified offset moves the input to the second stage away from the nominal DC operating point it was designed for.

4 Conclusion

Sensors produced by HPK will be used for the ATLAS ITk Strip detector. Defects arising during the fabrication process, such as metal or implant shorts between neighbouring strips, or shorts in the AC coupling of the readout chip to the strip implant, are expected to happen rarely. As long as the defects do not pose a risk to the operation of the readout chips as a whole, they will result in little to no losses in the tracking performance of the detector.

A study was performed to assess the electrical characteristics of sensor defects and whether they pose any risk to the operation of the front-end readout electronics. All of the studied defects were visible during electrical tests that will be performed during the module assembly procedure with the exception of pinholes. Pinhole channels were not visible for unirradiated sensors, but had a significant effect on the amplifier gain for irradiated sensors with leakage currents close to those expected at the end of their operational lifetime. The gain was observed to be affected beyond strip leakage currents of 250 nA, in agreement with simulation. The pinholes did not affect the read-out of neighbouring channels, and the chip response as a whole was unaffected. We conclude that pinholes do not pose a risk to module operations throughout their lifetime. Therefore, they do not require special handling during the module assembly, such as per-module custom wire-bonding maps or wire-bond removal. The identifiability of the other defects implies that the electrical testing procedure will be a reliable tool for characterizing the module performance during assembly.

The salient features of this study included silicon sensors with AC-coupling and poly-silicon biasing, operations in a radiation environment that raises the leakage current, the front-end amplifier with resistive feedback which is affected by the sensor current. Under these circumstances the voltage difference between the amplifier input and the implants affects the operational range in the experiment due to the portion of the current between the sensor electrode and the amplifier coming from the bias resistor. This voltage difference can be tuned at the module level by modulating the sensor potential. The results of the study should be relevant to other experiments employing the same technological features.

Acknowledgments

The research was supported and financed in part by the U.S. Department of Energy, Grant DE-SC0010107. We acknowledge the support of the Natural Sciences and Engineering Research Council of Canada (NSERC). We greatly appreciate the support and outstanding performance of the irradiation facilities. The proton irradiation was performed at the Cyclotron and Radioisotope Center (CYRIC) of Tohoku University in Japan. The neutron irradiation was performed at the Jožef Stefane Institute with the TRIGA Mark II Reactor in Ljubljana.

2021 JINST 16 P03037

References

[1] ATLAS collaboration, *Technical Design Report for the ATLAS Inner Tracker Strip Detector*, Tech. Rep. CERN-LHCC-2017-005; ATLAS-TDR-025 (2017).

[2] ATLAS collaboration, *Technical Design Report for the ATLAS Inner Tracker Pixel Detector*, Tech. Rep. CERN-LHCC-2017-021; ATLAS-TDR-030 (2017).

[3] V. Fadeyev et al., *Design and performance of silicon strip sensors with slim edges for HPS experiment*, *Nucl. Instrum. Meth. A* **969** (2020) 163991.

[4] F. Hartmann, *Evolution of Silicon Sensor Technology in Particle Physics*, *Springer Tracts Mod. Phys.* **275** (2017) 1.

[5] P. Rose, A.A. Grillo, V. Fadeyev, E. Spencer, M. Wilder and M. Domingo, *Simulation of the ATLAS SCT barrel module response to LHC beam loss scenarios*, 2014 *JINST* **9** C03012.

[6] H.F.W. Sadrozinski et al., *Punch-through protection of SSDs*, *Nucl. Instrum. Meth. A* **699** (2013) 31.

[7] J. Fernández-Tejero et al., *Beam-loss damage experiment on ATLAS-like silicon strip modules using an intense proton beam*, *Nucl. Instrum. Meth. A* **958** (2020) 162838.

[8] Y. Unno et al., *ATLAS17LS — A large-format prototype silicon strip sensor for long-strip barrel section of ATLAS ITk strip detector*, *Nucl. Instrum. Meth. A* (2020) 164928.

[9] K. Ambrozic, G. Zerovnik and L. Snoj, *Computational analysis of the dose rates at JSI TRIGA reactor irradiation facilities*, *Appl. Radiat. Isot.* **130** (2017) 140.

[10] L.B.A. Hommels et al., *Detailed studies of full-size ATLAS12 sensors*, *Nucl. Instrum. Meth. A* **831** (2016) 167.

[11] C.K. et al., *Initial tests of large format sensors for the ATLAS ITk strip tracker*, *Nucl. Instrum. Meth. A* **986** (2021) 164677.

[12] ATLAS ITk Strips collaboration, *Development of the ABCStar front-end chip for the ATLAS silicon strip upgrade*, 2017 *JINST* **12** C04017.

[13] ATLAS collaboration, *The ABC130 barrel module prototyping programme for the ATLAS strip tracker*, 2020 *JINST* **15** P09004 [arXiv:2009.03197].

[14] L.W. Nagel and D. Pederson, *SPICE (Simulation Program with Integrated Circuit Emphasis)*, Tech. Rep. UCB/ERL M382, EECS Department, University of California, Berkeley (1973).

2021 JINST 16 P03037